Materials Science-Poland, Vol. 25, No. 4, 2007

Synthesis and characterization of alumina nanopowders by combustion of nitrate-amino acid gels

M. EDRISSI[1], R. NOROUZBEIGI[1*]

[1]Chemical Engineering Department, Amirkabir University of Technology,
Hafez Ave., P. O. Box 15875-4413, Tehran, Iran

Nanocrystalline alumina powders were synthesized by the combustion method using serine and asparagine as fuels. A screening design was conducted to determine how key process factors influence preparation of nanocrystalline powders. The screening design was utilized to rank effective factors on crystalline size of alumina powders. The product was characterized by XRD, BET, and SEM. Nanocrystalline γ-alumina powders with crystal sizes between 3.95 nm and 6.71 nm and α-alumina powders with crystallite sizes between 22.73 nm and 33.92 nm have been obtained by the combustion synthesis. The specific surface areas of samples ranged between 22 m^2/g and 75 m^2/g. Particle size distributions were determined by LLS and the average particle sizes of γ-alumina powders after sonication were 37.42 nm and 79.32 nm. Results of statistical analysis illustrate that the fuel to oxidizer ratio is the most effective factor to decrease the average crystal size.

Key words: *alumina; combustion synthesis; screening design; serine; asparagine*

1. Introduction

Alumina is one of the most important ceramic materials widely used as electrical insulator, presenting exceptionally high resistance to chemical agents, as well as giving an excellent performance as catalyst or catalytic support for many chemical reactions [1, 2]. It is widely used for structural, microelectronic and membrane applications. Various chemical methods such as spray pyrolysis [3], precipitation [4], sol-gel [5], hydrothermal [6] and combustion synthesis [7] have been employed to synthesize ultrafine Al_2O_3 powders.

Combustion synthesis is a particularly simple, safe and rapid fabrication process wherein the main advantages are energy and time savings. This quick, straightforward process can be used to synthesize homogeneous, high-purity, crystalline oxide ceramic powders including ultrafine alumina powders with a broad range of particle sizes.

[*]Corresponding author, email: r_noroozbaigi@yahoo.com

The basis for the combustion synthesis comes from the thermochemical concepts used in the field of propellants and explosives [8]. The success of the process is due to an intimate blending among the constituents using a suitable fuel or complexing agent (e.g., citric acid [9], urea [10], glycine [11], etc.) in an aqueous medium and an exothermic redox reaction between the fuel and oxidizer (nitrates). Actually, the mechanism of the combustion reaction is quite complex. The main parameters influencing the reaction include type of the main fuel, fuel to oxidizer ratio, the amount of oxidizer in excess, ratio of fuels, pH of the solution and rate of calcination [12, 13]. In general, a good fuel should not react violently nor produce toxic gases, and must act as a complexing agent for metal cations [14]. In this research, two amino acids, serine ($HOCH_2CH(NH_2)COOH$) and asparagine ($NH_2COCH_2CH(NH_2)COOH$), were used as fuels. The effectiveness of important factors on the crystal size of combustion synthesized γ-alumina powders have been investigated using two-level factors in a screening design. The powders obtained through combustion synthesis were characterized by X-ray diffraction, surface area (BET), scanning electron microscopy (SEM), differential thermal analysis (DTA), thermogravimetric analysis (TG), and laser light scattering (LLS).

2. Experimental procedure

Design of experiments. A two level screening design was utilized for investigating and sorting the effective factors on combustion synthesis of alumina powders. The first step is selection of factors. The seven important factors studied are: the ratio of oxidizer in excess, type of fuel, fuel to oxidizer ratio, type of secondary fuels, secondary fuel to the main fuel ratio, pH of the starting solution and rate of calcination. The second step is determination of high and low levels for each factor. Ammonium nitrate (NH_4NO_3) was used as excess oxidizer (combustion aid) [15]. The molar ratio of ammonium nitrate to aluminum nitrate (main oxidizer) was selected as the first factor and amounts of 0.25 and 0.5 were its low and high levels, respectively. The initial composition of the solution containing aluminum nitrate, $Al(NO_3)_3{\cdot}9H_2O$ and asparagine was derived from the total oxidizing and reducing valences of the oxidizer and fuel using the concepts of propellant chemistry [16]. Carbon, hydrogen and aluminum were considered as reducing elements with the corresponding valences of +4, +1 and +3, respectively. Oxygen was considered as an oxidizing element with the valence of 2, the valence of nitrogen was considered to be 0. The total calculated valence of metal nitrates by arithmetic summation of oxidizing and reducing valences was –15. The calculated valence of asparagine was +18. The stoichiometric composition of the redox mixture demanded that $1(-15) + n(+18) = 0$, or $n = 0.833$ mol. This calculation was done for mixture of aluminum nitrate and serine, so the stoichiometric composition of the redox mixture demands that $1(-15) + n(+13) = 0$, or $n = 1.154$ mol. Selected levels for fuel to oxidizer ratio were stoichiometric amount (*St*) and $1.5\times St$. As mixtures of fuels can influence the final product size [12], we used mixtures of amino acids with

urea and ammonium acetate. In this study, the type of main fuels was a qualitative factor and asparagine and serine were high and low levels respectively; type of added fuel was another qualitative factor with assumption that urea is high level and ammonium acetate is low level, and the molar ratio of added fuel (urea or ammonium acetate) to the main fuel (serine or asparagine) was introduced as one of the quantitative factors. The amounts of 0 and 0.2 were selected as low and high levels, respectively. Other factors investigated were pH of the starting solution and rate of calcinations. The amounts 2 and 4 were chosen as low and high levels for the pH, which was adjusted by adding ammonium hydroxide or nitric acid to the solution. The 10 °C/min and 20 °C/min were selected levels for the calcination rate. The factors studied and the amounts used for high and low levels used in design of experiments are given in Table 1.

Table 1. Factors and levels

Factor	Allocated letter	High level	Low level
Molar ratio of the excess oxidizer to aluminum nitrate	A	0.5	0.25
Fuel to oxidizer ratio	B	1.5×*St*	*St*
Type of main fuel	C	asparagine	serine
Type of added fuel	D	urea	ammonium acetate
Molar ratio of added fuel to the main fuel	E	0.2	0
pH of the starting solution	F	4	2
Calcination rate	G	20 °C/min	10 °C/min

The combination of factors and levels according to screening design is given in Table 2.

Table 2. Screening design table

Sample	A	B	C	D	E	F	G
1	0.5	1.5	asparagine	urea	0.2	4	20 °C/min
2	0.5	1.5	serine	urea	0	2	10 °C/min
3	0.5	1	asparagine	ammonium acetate	0.2	2	10 °C/min
4	0.5	1	serine	ammonium acetate	0	4	20 °C/min
5	0.25	1.5	asparagine	ammonium acetate	0	4	10 °C/min
6	0.25	1.5	serine	ammonium acetate	0.2	2	20 °C/min
7	0.25	1	asparagine	urea	0	2	20 °C/min
8	0.25	1	serine	urea	0.2	4	10 °C/min

Preparation of samples. All materials used, supplied from the Merck Company (Germany), were reagent grade. Eight samples were prepared according to combination of

factors and levels shown in Table 2. In the first step, 0.04 mol of Al $(NO_3)_3 \cdot 9H_2O$ was dissolved in 100 ml of distilled water. The amounts of serine or asparagine with amounts of urea or ammonium acetate and consequent amounts of ammonium nitrate under vigorous stirring (700 r.p.m) were added to the solution. Then pH of the solution was adjusted with addition of ammonium hydroxide solution or nitric acid if required. The solution was then heated on a hot plate and stirred until the solution was boiled at 100 °C. When almost 90% of water evaporated, a yellowish and translucent gel was obtained. Then the obtained gel was transferred to a porcelain crucible, and was heated in a muffle furnace up to 400 °C and ignited at this temperature inside the muffle. At this stage a blackish voluminous fluffy solid product was obtained. It was calcined according to Table 2 up to 900 °C and remained at this temperature for 2 h. White and very fine powders were obtained. The powders were analyzed by X-ray diffraction (XRD) and average crystal sizes were selected as response of the experiments. X-ray diffraction was performed on calcined powders for phase characterization, at the rate of 1°/min, using nickel filtered CuK_α radiation in the 2θ range 25–80°, on a Philips X-ray diffractometer, (model X'Pert, Netherlands). The surface ares of the powders were measured using multipoint BET method (Quantachrome AutosorbI, Micromeritics instrument, USA) assuming a cross sectional area of 0.16 nm^2 for the nitrogen molecule. The porosity and the microstructure of the products were examined by means of scanning electron microscopy (Philips XL30, Netherlands). Thermal analyses were carried out on Shimadzu DTA-50 and Shimadzu TG-50 (Japan) up to 1200 °C with the rate of 10 °C/min. Particle size distribution was determined by laser light scattering (SEMATech model SEM33, USA).

3. Results and discussion

3.1. XRD data

As fuels, we have selected two amino acids with amino groups which may complex with metal cations and decompose at a relative low temperature giving ammonia (NH_3). The redox reaction between ammonia and the nitrogen oxides (NO_x) from the decomposed nitrates gives water and nitrogen:

$$4x\mathrm{NH}_{3(g)} + 10\mathrm{NO}_{x(g)} \rightarrow (5+2x)\mathrm{N}_{2(g)} + 6x\mathrm{H}_2\mathrm{O}_{(g)} + 2x\mathrm{O}_{2(g)} \quad (1)$$

The energy released from the redox reaction accelerates phase formation of γ-alumina [17].

The XRD patterns of powders calcined at 900 °C for 2 h are shown in Fig. 1. Pattern A shows the XRD pattern of sample 1 as-synthesized at 400 °C.

The peak broadening method was used to calculate the average crystallite size. The full width at half maximum (FWHM) of the peak was measured and the average crystallite sizes were estimated using the equation of Scherrer [18]:

$$D = \frac{0.9\lambda}{(\cos\theta)\sqrt{B^2 - b^2}} \tag{2}$$

where D is the average crystallite size, λ the wavelength of the radiation, θ Bragg's angle and B and b are the FWHMs observed for the sample and standard, respectively. Silicon powder was used to measure the instrumental peak broadening.

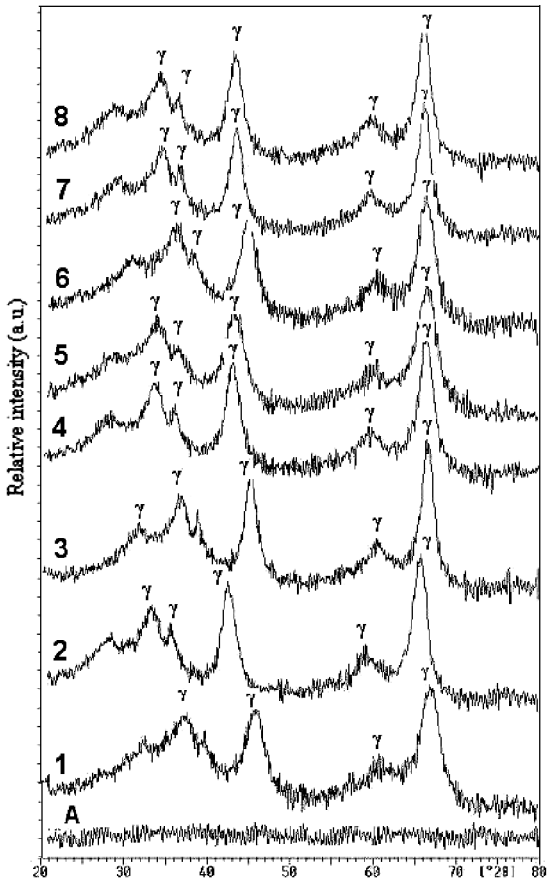

Fig. 1. XRD pattern of sample 1 as-synthesized (A) and samples 1–8 calcined at 900 °C

Terms B and 2θ were obtained from each XRD pattern and PC-APD (X_manager) software that uses information of ICDD (international centre of diffraction data) to recognize alumina phases. The average crystallite size for each sample was calculated from the above formula. Results are shown in Table 3.

The data of Table 3 demonstrate that sample 1 has the smallest average crystallite size (3.95 nm) and sample 7 has the largest one (6.71 nm). It should be mentioned that these results are almost the least average sizes that have been obtained by combustion synthesis.

Table 3. Bragg's angle, 2θ and average crystallite size of samples

Sample	B [deg]	B [rad]	2θ [deg]	Average crystal size D [nm]	Y_i (Response)
1	2.417	0.042184608	67.000	3.95	Y_1
2	1.809	0.030089476	66.872	5.29	Y_2
3	1.724	0.030089476	66.893	5.55	Y_3
4	1.861	0.032480577	66.780	5.14	Y_4
5	2.185	0.038135444	66.921	4.37	Y_5
6	2.241	0.039112828	66.648	4.26	Y_6
7	1.432	0.024993114	66.946	6.71	Y_7
8	1.750	0.030543261	66.830	5.47	Y_8

The pattern A in Fig. 1 confirms the amorphous structure and absence of crystalline phases in the as-synthesized powders. XRD patterns show that samples 1 and 5 have more amorphous particles than the others. Also the crystallinities of samples 2, 3, 6 and 7 are better than those of other samples. Furthermore, samples 2 and 3 are mixtures of δ and γ phases, and samples 6 and 7 are pure γ-alumina. Other samples are mixtures of γ-alumina crystalline powders containing some amorphous particles. The amount of gases released during the exothermic reaction is very high, so it cools the reaction environment. This results in poor crystallinity in some prepared powders. The results show that when an XRD profile has broad peaks, the crystallite sizes are small and the crystallinity is poor but when the peaks are narrow, the corresponding crystals are large. The mentioned software and XRD patterns show that all samples synthesized in this work are γ-alumina.

The effect of changing the level for anyone factor, E_f, is determined by subtracting the average responses (crystal size) when the factor is at its high level (L_+) from the average value when it is at its lower case level (L_-).

$$E_f = \frac{\left(\sum Y_i\right)_{\text{high level}}}{4} - \frac{\left(\sum Y_i\right)_{\text{low level}}}{4} \tag{3}$$

$$E_f = L_+ - L_- \tag{4}$$

$$E_A = \frac{Y_1 + Y_2 + Y_3 + Y_4}{4} - \frac{Y_5 + Y_6 + Y_7 + Y_8}{4} \tag{5}$$

$$E_B = \frac{Y_1 + Y_2 + Y_5 + Y_6}{4} - \frac{Y_3 + Y_4 + Y_7 + Y_8}{4} \tag{6}$$

$$E_c = \frac{Y_1 + Y_3 + Y_5 + Y_7}{4} - \frac{Y_2 + Y_4 + Y_6 + Y_8}{4} \tag{7}$$

$$E_D = \frac{Y_1 + Y_2 + Y_7 + Y_8}{4} - \frac{Y_3 + Y_4 + Y_5 + Y_6}{4} \tag{8}$$

$$E_E = \frac{Y_1 + Y_3 + Y_4 + Y_8}{4} - \frac{Y_2 + Y_4 + Y_5 + Y_7}{4} \tag{9}$$

$$E_F = \frac{Y_1 + Y_4 + Y_5 + Y_8}{4} - \frac{Y_2 + Y_3 + Y_4 + Y_7}{4} \tag{10}$$

$$E_G = \frac{Y_1 + Y_4 + Y_6 + Y_7}{4} - \frac{Y_2 + Y_3 + Y_5 + Y_8}{4} \tag{11}$$

Results of calculations are given in Table 4.

Table 4. Results of average calculations and term E_f for factors and optimum conditions to produce smaller particles

Factor	L_+	L_-	E_f	Comparison (smaller is better)	Optimum condition
A	4.9825	5.2025	–0.22	$L_+ < L_-$	increase of the factor quantity
B	4.4675	5.7175	–1.25	$L_+ < L_-$	increase of the factor quantity
C	5.1450	5.0400	0.105	$L_+ > L_-$	using serine
D	5.3550	4.8300	0.525	$L_+ > L_-$	using ammonium acetate
E	4.8075	5.3775	–0.57	$L_+ < L_-$	increase of the factor quantity
F	4.7325	5.4525	–0.72	$L_+ < L_-$	increase of the factor quantity
G	5.0150	5.1700	–0.155	$L_+ < L_-$	increase of the factor quantity

As we are looking for the production of smaller particles, the least average is considered as the aim of calculations. By utilizing this concept, the optimum condition of factors to produce smaller particles is obtained and it is also given in Table 4.

Sorting of the amounts of E_f without consideration of their signs leads to ranking of factors based on their influence on the combustion synthesis of alumina. Results are given in Table 5.

Factor B (fuel to oxidizer ratio) is the most important factor responsible for reducing the average diameter value of γ-alumina. This result agrees with other reports of nanoalumina combustion synthesis [7]. Other effective factors are F (pH of the solution) and E (molar ratio of added fuel to the main fuel), respectively. Adjustment of pH was done by addition of nitric acid or ammonium hydroxide. Addition of these materials would change the concentration of nitrate ions, and it can change the amount

of fuel to oxidizer ratio. The increase of nitrate ions in the low pHs is expected to decrease the enthalpy of exothermic reaction by decreasing the fuel to oxidizer ratio. Thus the rate of combustion reaction would decrease and in this condition alumina particles come closer to foam structure and agglomeration will increase [9].

Table 5. Ranking of factors (screening) based on sorting the $|E_f|$ values

Ranking of the factors	$\|E_f\|$
1 – fuel to oxidizer ratio	1.25
2 – pH of the starting solution	0.72
3 – molar ratio of added fuel to the main fuel	0.57
4 – type of added fuel	0.525
5 – molar ratio of the excess oxidizer to aluminum nitrate	0.22
6 – calcination rate	0.155
7 – type of main fuel	0.105

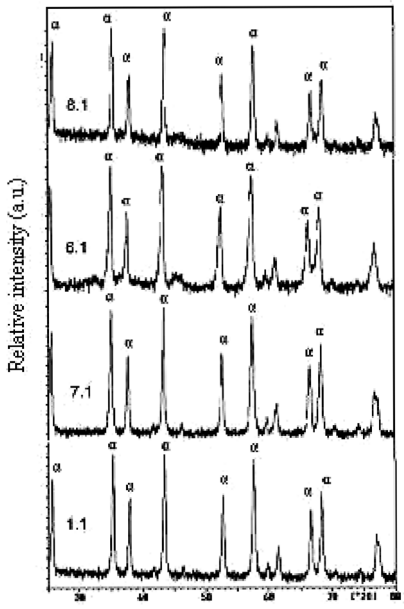

Fig. 2. XRD patterns of powders 1.1, 7.1, 6.1 and 8.1

The effect of D (type of added fuel) is positive, hence in comparison with urea, ammonium acetate fuel is more suitable. Using urea as a fuel leads to a flaming type combustion. When flame persists for a longer time, the particles have enough time and temperature to sinter and thus yield larger particles [14]. The effects of A, G, and C are less important and the least effective factor is C (type of the main fuel). In this research, we selected two similar fuels. These fuels are amino acids, so their influence

on the combustion reaction is almost similar. Differences in organic structure of fuels would make the factor C one the more effective factors of combustion synthesis [11].

In the Table 3, powders 1 and 7 have the lowest and highest responses of alumina production from asparagine, and powders 6 and 8 have the lowest and highest responses of alumina production from serine, respectively; the powders which previously were calcined at 900 °C for 2 h were again calcined from ambient temperature up to 1100 °C and maintained at this temperature for 2 h. Resulting products obtained from powders 1, 6, 7, and 8, were named 1.1, 6.1, 7.1, and 8.1 respectively. Figure 2 shows the XRD patterns of the products. XRD patterns show that all these products are α-alumina. The average crystallite sizes for each powder were calculated by Scherer's formula. The results are given in Table 6.

Table 6. Average crystallite sizes of powders calcined at 1100 °C

Powder number	Average crystallite size [nm]
1.1	33.41
6.1	22.73
7.1	33.92
8.1	25.92

Values of Table 6 show that α-alumina powders with average crystallite sizes between 22.73 and 33.92 nm have been obtained. The crystal sizes increased when calcined at 1100 °C. These results demonstrate that the dimensions obtained by us are smaller than those of α-alumina powders previously produced by other fuels like citric acid, glycine, urea, ammonium acetate, etc. [7]. The results show that serine and asparagine are suitable fuels for combustion synthesis of α-alumina nanostructured powders.

3.2. BET Data

The specific surface areas of samples 1 and 6 were calculated according to the Brunnauer–Emmet–Teller (BET) procedure [19] by using the data of adsorption of nitrogen on the samples at 77 K assuming the cross sectional area of 0.16 nm^2 for the nitrogen molecule. The results show that the specific surface area of sample 1 is 22 m^2/g and the specific surface area of sample 6 is 75 m^2/g. Thus the specific surface area of the sample produced by serine-nitrate combustion is higher than that of the sample being the product of asparagine-nitrate combustion. The surface areas of samples show that these samples are suitable for using as catalyst supports or adsorbents.

3.3. DTA/TG data

The DTA and TG analyses were also performed on sample 6 to investigate the phase transformations. In Fig. 3, the TG curve demonstrates two weight loss steps.

First, it was verified on a significant fall by about 22% at 500 °C. The second drop was slight by about 3% at 1100 °C. Afterwards the curve became horizontal. With DTA analysis it was possible to confirm phase transformation into thermodynamically stable crystallographic alpha alumina at about 1100 °C. This result agrees with that obtained by XRD Analyses. Actually, the temperature of phase transformation is identified on the same manner.

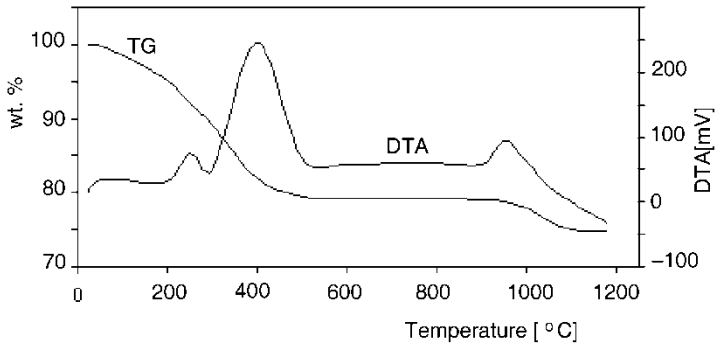

Fig. 3. DTA/TG curves of sample 6

3.4. SEM data

A Phillips XL30 electron microscope was used to take SEM view of the samples 1 and 6 (magnification 50 000×). The SEM photographs of the samples are given in Fig. 4. It was clearly observed from these photographs that sample 6 has a higher porosity and surface area than sample 1. The porosity range of sample 6 is 50–250 nm and could be used as a molecular sieve or a catalyst support [20, 21].

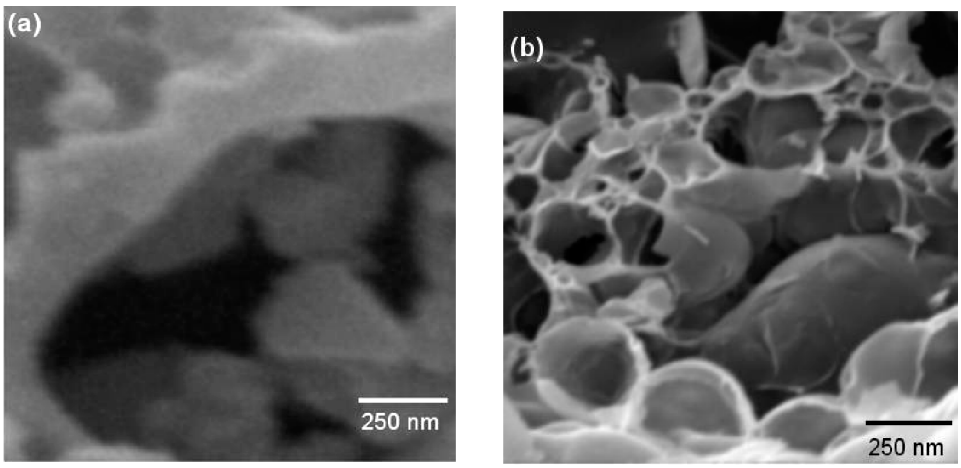

Fig. 4. SEM photographs of the sample 1 (a) and sample 6 (b)

3.5. LLS data

The corresponding particle size distributions of samples 1 and 6 were obtained with laser light scattering in dilute aqueous suspensions after ultrasonic deagglomeration. Results are shown in Figs. 5 and 6. The average particle size of sample 1 was 37.42 nm and the average particle size of sample 6 was 79.32 nm. Particle sizes obtained by combined combustion synthesis and sonication are lower than 100 nm and show success of the method for producing nanopowders. Furthermore, the particle size distribution profiles are narrow and two distributions are homogeneous.

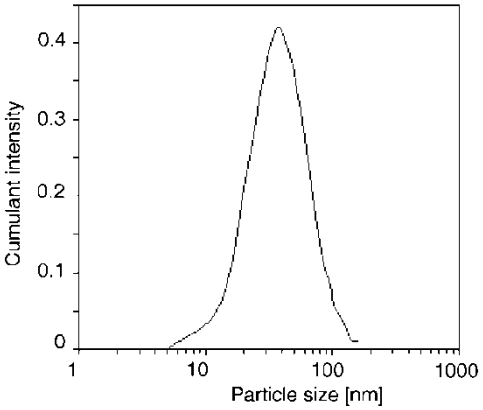

Fig. 5. Particle size distribution of sample 1 after sonication

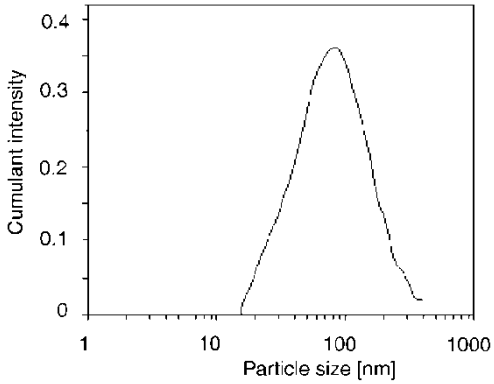

Fig. 6. Particle size distribution of sample 6 after sonication

4. Conclusion

In this research, γ-Al_2O_3 nanopowders with crystallite sizes between 3.95 nm and 6.71 nm and α-alumina with crystal sizes between 22.73 nm and 33.92 nm were successfully synthesized by using serine and asparagine as new fuels. The average particle sizes of γ-alumina powders after sonication were 37.42 nm and 79.32 nm. These results show that serine-nitrate and asparagine-nitrate gel combustion syntheses have outstanding potential for producing nanocrystalline alumina powders in comparison with other conventional fuels.

Using a screening design, the order of effective factors and the optimum combination of their levels required for preparing γ-Al_2O_3 with consideration of smaller crystal sizes was obtained, so the most effective factor was fuel to oxidizer ratio. The specific surface areas of powders were measured and the results show that specific surface areas of samples produced from serine-nitrate combustion are larger than those of samples prepared from asparagine-nitrate combustion.

References

[1] MACEDO M.I.F., OSAWA C.C., BERTRAN C.A., J. Sol-Gel Sci. Techn., 30 (2004), 135.
[2] ADA K., SARIKAYA Y., ALEMDAROGLU T., ONAL M., Ceram. Intern., 29 (2003), 513.
[3] VARATHARAJAN K., DASH S., ARUNKUMAR A., NITHYA R., TYAGI A.K., RAJ B., Mater. Res. Bull., 38 (2003), 577.
[4] SHARMA P.K., VARADAN V.V., VARADAN V.K., J. Europ. Ceram. Soc., 23 (2003), 659.
[5] DUMEIGNIL F., SATO K., IMAMURA M., MATSUBAYASHI N., PAYEN E., SHIMADA H., Appl. Catalysis A: General, 241 (2003), 319.
[6] QU L., HE C., YANG Y., HE Y., LIU Z., Mater. Lett., 59 (2005), 4034.
[7] LI J., PAN Y., XIANG C., GE Q., GUO J., Ceram. Intern., 32 (2006), 587.
[8] FUMO D.A., MORELLI M.R., SEGADAES A.M., Mater. Res. Bull., 31 (1996), 1243.
[9] PATHAK L.C., SINGH T.B., DAS S., VERMA A.K., RAMACHANDRARAO P., Mater. Lett., 57 (2002), 380.
[10] BHADURI S., ZHOU E., BHADURI S.B., Nanostruct. Mater., 7 (1996), 487.
[11] TONIOLO J.C., LIMA M.D., TAKIMI A.S., BERGMANN C.P., Mater. Res. Bull., 40 (2005), 561.
[12] ARUNA S.T., RAJAM K.S., Mater. Res. Bull., 39 (2004), 157.
[13] PENG T., LIU X., DAI K., XIAO J., SONG H., Mater. Res. Bull., 41 (2006), 1638.
[14] KINGSLEY J.J., PEDERSON L.R., J. Mater. Res. Soc. Symp. Proc., 296 (1993), 361.
[15] BURGOS-MONTES O., MORENO R., COLOMER M.T., FARINAS J.C., J. Europ. Ceram. Soc., 26 (2006), 3365.
[16] JAIN S.R., ADIGA K.C., Combust. Flam., 40 (1981), 71.
[17] LI F., HU K., LI J., ZHANG D., CHEN G., J. Nucl. Mater., 300 (2002), 82.
[18] BIAMINO S., FINO P., PAVESE M., BADINI C., Ceram. Intern., 32 (2006), 509.
[19] SARIKAYA Y., ADA K., ALEMDAROGLU T., J. Europ. Ceram. Soc., 22 (2002), 1905.
[20] PARK J.-Y., OH S.-G., PAIK U., MOON S.-K., Mater. Lett., 56 (2002), 429.
[21] ZHU H.Y., RICHES J.D., BARRY J.C., Chem. Mater., 14 (2002), 2086.

Received 24 February 2007
Revised 11 August 2007